The Effect of Shear on the Crystallization of Cocoa Butter

S. Sonwai* and M.R. Mackley

Department of Chemical Engineering, University of Cambridge, New Museums Site, Cambridge, England CB2 3RA

ABSTRACT: This paper examines the effect of shear on the crystallization of cocoa butter using a combination of three different experimental techniques and a single crystallization temperature of 20°C. Rheological measurements were carried out to study the effect of a shear step on the crystallization kinetics of the fat. Without a shear step, little rheological change was observed at 20°C; however, with the application of a shear step the onset of significant rheological change occurred and was strongly influenced by the magnitude of the shear step. Detailed crystallographic measurements could be made with *in situ* X-ray experiments during flow-induced crystallization. The imposition of continuous shear changed both crystal polymorphic structure and crystallization kinetics in a systematic way. Finally, optical measurements were used to follow changes in crystal morphology as a consequence of continuous shear. These results revealed the form and kinetics of crystal growth. In general the results complemented each other, and an overall picture of the way shear influenced cocoa butter growth could be formed. The observations could be the basis for a future mathematical model of growth kinetics and provide insight into the way shear influences crystallization kinetics, morphology, and polymorphic structure.

Paper no. J11229 in *JAOCS 83*, 583–596 (July 2006)

KEY WORDS: Cocoa butter, crystallization, crystallization kinetics, morphology, polymorphism, rheology, shear, X-ray diffraction.

Cocoa butter (CB) is a semisolid fat that exhibits brittleness below 20°C, begins to soften in the region of 28–32°C, and melts completely below body temperature (1). CB is predominantly composed of three monounsaturated TAG—POP, POS and SOS (where P = palmitate, O = oleate, and S = stearate)—which make up approximately 82% of its components (2). It also contains minor concentrations of MAG, DAG, phospholipids, glycolypids, sterols, FFA, and fat-soluble vitamins. The TAG composition of CB from cocoa beans grown in different areas varies slightly according to differences in genetics, climate (temperature, rainfall, and sunlight), and agricultural practices.

CB, which itself is tasteless (1), is a key ingredient in chocolate. It typically corresponds to approximately one-third of the chocolate composition. Because of this, the crystallization of CB plays an essential role in controlling the physical and thermal properties of chocolate products. The crystallization behavior of CB is, however, very complex owing to polymorphism, i.e., the ability of the fat to exist in different crystalline forms with different types of crystal packing and thermodynamic stabilities (3). It is now generally accepted that CB can exist in six polymorphs, which in order of increasing thermodynamic stability are termed Form I–Form VI (4). Only Form V is used by the confectionery industry as the optimal polymorph for CB in chocolate (5). This is because Form V is a stable polymorph with a melting range that is high enough to allow chocolate to be stored at room temperature, and low enough that chocolate becomes a smooth liquid when it is heated in the mouth. Form V provides chocolate products with snap (ability to break apart easily), good demolding properties (contraction), and a good quality finish in terms of color and gloss. Moreover, Form V exhibits resistance to fat bloom, which is a physical defect that appears during storage as undesirable white spots or a streaky grey-white finish on the chocolate surface (6). One of many causes for fat bloom is phase transformation of CB from an unstable form to the more stable one during storage (1,5). This happens when CB in chocolate is not properly solidified and hence crystallizes into an unstable form. Accordingly, Form V of CB is promoted during chocolate crystallization. Unfortunately, Form V is not readily obtained in the bulk of chocolate by simple cooling, but rather by using a tempering protocol that is aimed at having sufficient CB crystal seeds of stable polymorph to nucleate the bulk of the remaining fat into the stable form (Form V). During tempering, the chocolate mixture is subjected to a well-controlled temperature program under the action of shear or flow from mixing. Temperature control is vital for the tempering process. The actual temperatures required to temper chocolate vary depending on the types of the tempering machines and the fat phase composition of the chocolate. The contribution of shear during mixing is important but not well understood. A better understanding of the mechanism underlying the influence of shear on the crystallization of CB could result in both process and product enhancement.

A number of studies on the effect of shear on the crystallization of CB have been conducted. In 1962, Feuge *et al.* (7) was the first to report a solid-to-solid transformation of CB from a less stable form (Form II) to the more thermodynamically stable one (Form V) by mechanical work consisting of repeated extrusion under pressure (≤1000 psi). MacMillan *et al.* (8) used X-ray diffraction technique in small-angle scattering to study the crystallization of CB at 20–28°C with continuous shear rates of 0–12 s^{-1}. At 20°C in particular and with all shear rates, the fat was found to crystallize initially in Form III before

*To whom correspondence should be addressed at Dept. of Food Technology, Faculty of Engineering and Industrial Technology, Silpakorn University, Nakorn Prathom, 73000, Thailand. E-mail: ssonwai@su.ac.th

transforming to Form V, with the absence of Form IV. The induction time of Form V was found to decrease as the applied shear rate increased. However, the identification of Form III as an initial nucleating phase using small-angle scattering technique was ambiguous because Forms II and III exhibit similar diffraction characteristics in the small-angle region (4). Mazzanti *et al*. (9) proposed that the shear-induced acceleration of phase transformation from a less stable to more stable polymorphic forms was universal among three major commercial fats: CB, milk fat, and palm oil. By using X-ray diffraction technique in both small- and wide-angle scattering, the initial nucleating phase for the crystallization of CB at 18°C with continuous shear rate of 1440 s^{-1} was identified as Form III, which rapidly transformed into Form V at a later stage, bypassing Form IV. However, the possibility of Form II coexisting with Form III at these early stages of crystallization was not completely ruled out. The same authors (10) reported a similar phenomenon of shear-induced phase transition of CB. However, in using mainly the small-angle scattering technique, the initial nucleating phase of the sample crystallized at 20°C with continuous shear rates of 90 and 720 s^{-1} was tentatively referred to as Form II. Interestingly, the phase transition from Form II to V at a shear rate of 720 s^{-1} was observed going through a structure that exhibited a similar diffraction characteristic in the small-angle region to that of Form IV. In addition, it appeared that the induction time of Form V was higher at a shear rate of 720 s^{-1} compared with a shear rate of 90 s^{-1}, and this observation contradicted the previous report by MacMillan *et al*. (8). The influence of shear on the crystallization kinetics of CB was also investigated by Ziegleder (11), who reported a decrease in the crystallization induction time as the magnitude of the shear applied to the fat during crystallization at 21–29°C increased.

In this paper, the effect of shear on the crystallization kinetics, polymorphic behavior, and crystal morphology has been systematically investigated at a single temperature of 20°C using three different experimental techniques. First, a rheological viscoelastic test was used to study the effect of a steady shear step, applied for a short interval (250 s) during crystallization, on the crystallization kinetics of CB. The use of a rheological measurement as a probe for studying shear-induced crystallization kinetics of CB has been reported previously (12,13), but these experiments were carried out with continuous shear applied throughout the whole experiment. It is generally agreed that the solid content of fats is the major factor determining their rheological behavior (14). Second, the effect of continuous shear on the polymorphic behavior of CB was investigated using a Rheo-X-Ray facility, which combines a specially designed capillary rheometer with an X-ray powder diffraction facility (15). The Rheo-X-Ray facility allowed *in situ* observation of the evolution of individual crystal forms and of simultaneous rheological change of CB under highly controlled shear and temperature ranges for an extended time. Finally, the influence of continuous shear on the crystal morphology and crystallization kinetics of CB was observed through a purpose-built polarized light optical microscope (16), the sample stage of which was equipped with a shear cell. The results from each of the experimental techniques were then linked, and a qualitative physical picture of the overall behavior of the CB system was developed.

EXPERIMENTAL PROCEDURES

Material. The CB used was a standard factory product that originated in the Ivory Coast and was kindly supplied by Nestlé PTC (York, England).

The effect of shear step on the crystallization kinetics of CB. Studies in this section used a Rheometrics Dynamic Spectrometer [RDS II; Rheometrics (now part of TA Instruments Ltd., Manor Royal Crawley, West Sussex, England)], which is a controlled strain rheometer consisting of a stationary top plate and a moving bottom plate (17). To probe rheological changes during the crystallization of CB at 20°C under both static and shear step conditions, small-strain oscillatory measurements (called "dynamic time sweep measurements") were carried out. These oscillatory measurements measured the dynamic moduli (G', G'') and the complex viscosity (η^*) at a small deformation of 10% strain and a fixed frequency of 10 rad/s. The measurements used a (2000 g·cm) Force Rebalance Transducer and the 25-mm parallel plate configuration with 0.5-mm gap width. The temperature and shear regime is given in Figure 1. The fat was melted at 60°C for 10 min during time **a** using a hot plate. This was performed to ensure a complete melting of the fat, thereby preventing it from being influenced during crystallization by any memory effect. A molten fat is generally freed from the memory effect when it is heated for a few minutes at 20–30°C above the melting temperature of the stable variety (18). Then, 1 mL of the molten sample was transferred, during time **b** (which lasts for 40 s), to the sample stage of the RDS II, the temperature of which was set to 20°C. Oscillatory dynamic time sweep tests started at **c** ($t = 0$) and lasted for 200 s, during which G', G'', and η^* were measured. Then, the measurements stopped for 250 s in **d** (called a pause period), during which the sample was either at rest (for the experiments under quiescent conditions) or subjected to a constant shear step (for experiments under shear conditions). The chosen shear rates were be-

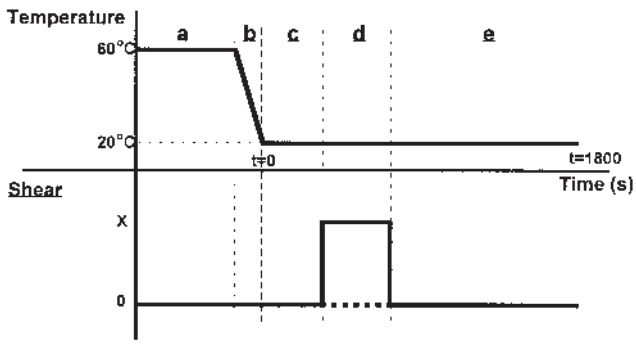

FIG. 1. The temperature and shear regime for crystallization experiments of cocoa butter (CB) at 20°C under static and shear conditions using the Rheometrics Dynamic Spectrometer (RDS II). X represents magnitude of shear rate.

tween 50 and 1500 s^{-1}. However, considering the parallel plate geometry of the RDS II, the material would be subjected to a broad range of shear rates, the average of which being much less than the nominal values presented here. The dynamic time sweep measurements resumed during time **e** until $t = 1800$ s or until the monitored G', G'', and η^* reached the high torque limit of the machine.

The effect of continuous shear on the polymorphic behavior of CB. Investigation of the way that continuous shear influenced the polymorphic behavior of CB was achieved by using a Rheo-X-Ray facility, which combines a specially designed capillary rheometer (called the Multipass Rheometer or the MPR III; Department of Chemical Engineering, University of Cambridge, Cambridge, England, in collaboration with Eland Test Plant, Walton-on-Thames, Surrey, England), with an X-ray powder diffraction facility (15). The MPR III is a twin-piston capillary rheometer that consists of a top and bottom barrel through which two pistons enter the system. In between the barrels is a test section that contains a beryllium capillary. The advantage of this apparatus over conventional capillary rheometers is that the sample is fully enclosed at a controlled temperature and pressure. The maximum range of shear rates applied to the sample can be high and similar to, or greater than, those used during industrial processing. The shear rate is a function of the piston volumetric flow rate, which is in turn a function of the piston velocity. For a Newtonian fluid with no-slip boundary condition, the apparent wall shear rate ($\dot{\gamma}$) is given by Equation 1 (19):

$$\dot{\gamma} = \frac{4Q}{\pi a^3} \qquad [1]$$

where a is a capillary radius and Q is the volumetric flow rate, which is defined as $\pi R^2 V_p$, where V_p is the piston velocity and R is the piston radius. The shear rate obtained from Equation 1 is computed at the inner wall of the capillary. Therefore, the value represents the maximum possible shear rate (called "wall shear rate"), which decreases to zero at the axis in an ideal laminar flow. This means that the material contained inside the test section of the MPR III is subjected to a range of shear rates, rather than one value alone. Details on the general operation of the MPR III are given in Mackley *et al*. (20).

The X-ray facility consists of a commercial Siemens Kristalloflex 760 X-ray generator and a Siemens HI-Star detector with a circular active area of diameter 115 mm. The X-ray generator consists of a sealed tube containing a copper anode and is able to generate X-ray radiation up to a power of 2.2 kW. The generated X-rays passed through a graphite monochromator to give a 1.5418 Å beam that was localized before it impinged on the sample by using a collimator of 0.8 mm in diameter, allowing the beam to probe through the regions with different shear rates from the wall to the center; the observed diffraction patterns resulted from the superposition of all those different hydrodynamic conditions. The sample–detector distance was varied between 125 and 764 mm, enabling a structure characterization of materials with a wide range of periodicities (typically from 3 to 200 Å, depending on the size of the beam stop used). By varying the sample–detector distance and the detector swing angle, the sample characterization was performed in either small-angle X-ray scattering (SAXS) or wide-angle X-ray scattering (WAXS) modes. Details for the SAXS and WAXS settings of the Rheo-X-Ray facility are presented in Reference 15. The dimensions of the berillium capillary used with the MPR III were diameter 4 mm and length 10 mm. During operation of the Rheo-X-Ray facility, the MPR III acted as a flow device by operating in the "multipass steady mode." The sample inside the test section was driven in alternating directions, with a constant piston velocity through a capillary insert, thereby creating a "steady" shear rate over an extended period. The pressure difference across the capillary was continuously obtained from the difference in the pressure values recorded from both ends of the capillary.

The crystallization of CB at 20°C was followed under both quiescent and continuous multipass shear conditions, utilizing mainly the SAXS mode. Whenever additional information in WAXS was required to identify the sample structure unambiguously, the experiment would be repeated in the WAXS mode. The sample–detector distances were 763 and 180 mm for the setup in SAXS and WAXS, respectively. The experiments began with melting solid CB in the test section at 60°C for 30 min before cooling it to 20°C. The melting time was longer for this experimental technique than the previous one since the amount of the sample contained in the test section was higher. A period of 30 min would be sufficient for every part of the sample inside the test section to reach 60°C for more than a few minutes, hence erasing all memory effect, before the temperature was lowered. The experiment under quiescent conditions was carried out without piston movement. For the crystallization with shear, the sample was kept under static conditions as it was cooled from 60 and 35°C. Once the temperature had reached 35°C, a steady shear was applied to the sample continuously from this point until the experiment ended. The selected piston velocities were 7, 15, 20, 50, and 250 mm/s, which, by using Equation 1, corresponded to maximum wall shear rates of 84, 180, 240, 600, and 3000 s^{-1}, respectively. The cooling rate was 3–5°C/min during cooling from 60 to 22°C, after which it was automatically reduced to <0.5°C/min until the temperature reached 20°C in order to avoid temperature undershoot. The crystallization of the sample could begin at any point during the period of slow cooling. Therefore, the timing was set to start ($t = 0$) and the data collection began once the temperature reached 20.5°C, after which the temperature fell gradually and reached 20°C within 5 minutes. The crystallization time was 60–70 min. X-ray data collection was performed once per minute, and each X-ray exposure time was 50 s. Only during experiments with shear was the pressure difference across the capillary continuously recorded. The pressure difference across the capillary is directly related to the apparent viscosity of a Newtonian fluid sample (19).

The effect of continuous shear on the crystal morphology and the crystallization kinetics of CB. A purpose-built optical microscope was used to observe the effect of continuous shear. The sample stage of the microscope was equipped with a shear

cell called the Cambridge Shear System (CSS450; Department of Chemical Engineering, University of Cambridge, Cambridge, England, in collaboration with Linkam Scientific Instruments, Tadworth, Surrey, United Kingdom). The microscope has a high-resolution temperature control, and one of the two optical discs mounted on the center of the CSS450 can be rotated with respect to the other either in steady or oscillatory motion; details of the apparatus have been described by Mackley *et al*. (16). CB was crystallized under both quiescent and shear conditions at 20°C. The chosen shear rates were 0, 3, 20, 100, 300, and 500 s^{-1}, with an 80 mm gap width. All experiments began with loading 0.5 mL of liquid CB (preheated at 60°C) into the sample stage of the CSS450. Then the liquid sample was heated to 80°C for 10 min, after which it was cooled to 50°C at 10°C/min. The temperature was immediately reduced further at 5°C/min to 20°C. Then, timing started (t = 0), and the temperature was maintained at 20°C for at least 60 min. It was not possible to use the same cooling rates as used in the experiments with the Rheo-X-Ray facility because the two apparatus had different cooling systems with different capabilities. For the crystallization under quiescent conditions the sample was not subjected to shear throughout the experiment. For the crystallization with a continuous shear, no shear was applied to the sample during cooling between 80 and 35°C. When the temperature reached 35°C, a continuous shear was applied to the sample and the shearing continued until the experiments ended. The crystallization of the sample at 20°C was continuously recorded onto S-VHS videotape through a 20× objective under polarizing conditions. Due to the high rotational speed of the bottom disc while the material was subjected to a steady shear in the experiments under shear conditions, the recording of the optical data onto S-VHS videotapes would result in captured images with poor quality. To resolve this problem, the applied shear rate was rapidly reduced to and maintained at 0.5 s^{-1} for 10 s at the beginning of every minute, during which the results were continuously recorded onto the videotape. After the 10 s, the shear rate was brought immediately back to the normal amplitude. The optical data were converted from videotapes to digital files and captured into frames using image analysis software. Then, the images were greyscaled and put through the same level of contrast enhancement.

RESULTS AND DISCUSSION

The effect of shear step on the crystallization kinetics of CB. The changes in the rheological parameters G', G'', and η* as a function of time during the crystallization of CB at 20°C for quiescent conditions and with a steady shear step of 50 s^{-1} are given in Figures 2a and 2b, respectively. For quiescent conditions, Figure 2a shows that, during the isothermal holding time **c**, the values of G', G'', and η* were low and fluctuating, and the viscous modulus G'' dominated over the elastic modulus G'. Near the end of time **c**, G', G'', and η* increased slightly. It is likely that this slow increase in the rheological parameters was associated with the onset of a primary-phase crystallization of CB. After being at rest during the pause period **d**, an increase in G', G'', and η* was

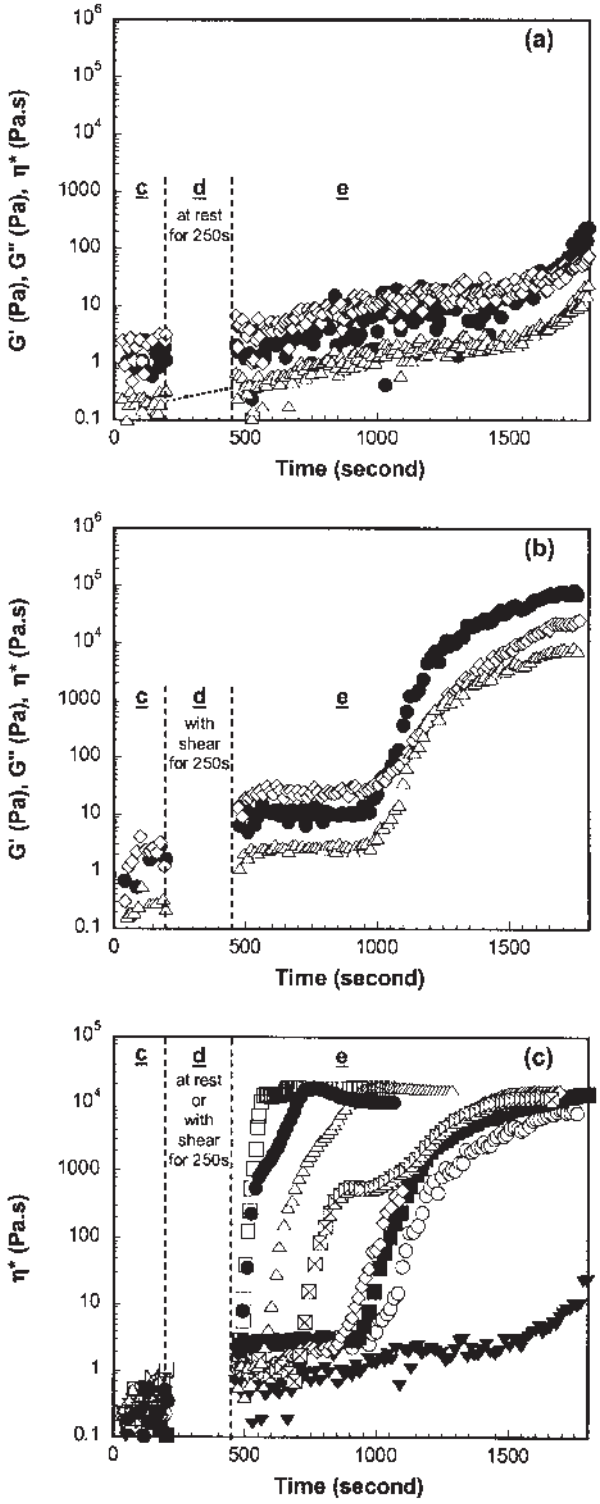

FIG. 2. The change in the rheological parameters G' (●), G'' (◇), and η* (△) as a function of time during the crystallization of CB at 20°C: (a) under quiescent conditions, (b) with shear step rate 50 s^{-1} (data obtained from the dynamic time sweep measurements using the RDS II), (c) changes in complex viscosity, η*, during the crystallization of CB at 20°C as influenced by various shear step rates. (▼, no shear; ○, shear rate 50 s^{-1}; ■, shear rate 100 s^{-1}; ◇, shear rate 500 s^{-1}; open box with superimposed ×, shear rate 800 s^{-1}; △, shear rate 1000 s^{-1}; ●, shear rate 1200 s^{-1}; □, shear rate 1500 s^{-1}). See Figure 1 for abbreviations.

apparent during the early stage of time **e**, where G'' was still dominant over G'. The dotted line connecting the η* data between times **c** and **e** demonstrates that the rheological measurement did not alter the crystallization kinetics of the sample. At t = 1600 s, G', G'', and η* started to increase more steeply and then G' became dominant over G'', indicating that the sample had become more solid-like as the amount of the fat crystals increased. The sample looked slightly turbid at the end of the experiment.

Figure 2b shows data where shear is involved. During time **c**, the sample exhibited the same rheological behavior as in the experiment under quiescent conditions. Again, a slow increase in G', G'', and η* during time **c** was possibly related to the onset of some primary-phase crystallization of the sample. After the period of 250 s where a steady shear rate of 50 s^{-1} was applied, there was a significant increase in G', G'', and η* in time **e** from time **c**, indicating that the fraction of crystallized sample at this point was higher when compared with the experiment under static conditions. η* increased substantially from well below 1 Pa·s to higher values. The domination of G'' over G' can still be seen during the time between 500 and 1000 s. However, after t = 1000 s, G', G'', and η* increased dramatically with a higher rate of change compared with the crystallization without shear (at $t \geq 1600$ s). When the experiment ended at t = 1800 s, the sample was turbid. The results shown in Figures 2a and 2b indicate that the onset of crystallization, as indicated by rheological change, took place within 100—150 s after the temperature had reached 20°C, leading to a slow increase in the rheological parameters. A secondary modification in rheological change, presumably associated with further secondary-phase crystallization, occurred earlier for the crystallization with a shear step (at t = 1000 s) compared with no shear (at t = 1600 s).

The overall effect of the steady shear step on the crystallization kinetics of CB can be seen clearly in Figure 2c, which shows the changes of complex viscosity, η*, of CB during crystallization with shear steps of magnitudes ranging from 0 to 1500 s^{-1}. The viscosity in all experiments increased continuously with time as the primary-phase fat crystallized. Without shear, η* climbed slowly throughout 1800 s of the experimental time, with a slightly higher rate toward the end. We associate this increase with some form of primary crystallization. With the application of steady shear step, η* increased slowly at first but much more rapidly at a later stage due to a second-phase crystallization. The higher the shear rate applied, the earlier η* started to make a rapid climb.

It is well known that suspended particles influence the flow behavior of a fluid. The increase in viscosity of the sample during crystallization can be related to the increase in the amount of the fat crystals present and thus to the degree of crystallinity. A steady shear step applied to the sample for only a short time during the crystallization substantially accelerated an apparent secondary crystallization process of CB. The onset of the major increase in complex viscosity occurred earlier in time with increasing applied steady shear step, indicating that the sample crystallized faster and with higher level of crystallinity. The influence of shear step on the crystallization kinetics of CB observed in this work through the rheological measurement was similar to the way that continuous shear affected the crystallization kinetics of CB at the same temperature observed by Dhonsi and Stapley (13) and at 19°C by Toro-Vazquez *et al*. (12). Both reported an increase in a rheological parameter (viscosity for the former, torque for the latter) as an onset of crystallization took place, and an increase in the applied shear rate resulted in shorter crystallization induction times.

The effect of continuous shear on the polymorphic behavior of CB. Figure 3 shows typical 2-D X-ray diffraction images and the corresponding diffraction plots in both SAXS and WAXS regions of CB crystallized at 20°C without shear (Fig. 3a) and with shear rate 84 s^{-1} (Fig. 3b). The diffraction plots were derived from radial intensity averaging of the diffraction images captured by the detector. Without shear, between the crystallization times of 0 and 60 min, the diffraction profiles of the sample exhibited one diffraction peak in SAXS at 1.8°2θ, corresponding to a d-spacing of 49 Å, and a small diffraction peak in WAXS at 20.95°2θ (4.24 Å). These are the diffraction characteristics of CB in Form II (4). Although the diffraction peak at 4.24 Å seen in WAXS could be misinterpreted as the strongest diffraction peak of Form III at 4.25 Å due to the proximity of their locations, the other three diffraction peaks of Form III in WAXS at 4.92, 4.62, and 3.86 Å reported in the literature (4) were not detected. After 60 min, the position of the diffraction peak in SAXS began gradually to move outward, changing from 1.8°2θ to 1.86°2θ (47.5 Å) at 70 min. At the same time, changes were also detected in the WAXS area with the diffraction peak at 20.95°2θ fading away and two new peaks appearing at 20.4°2 (4.35 Å) and 21.4°2θ (4.15 Å), diffraction characteristics in WAXS of Form IV. This modification of the diffraction pattern in both SAXS and WAXS indicates that the polymorphic structure of the sample was in the process of transforming from Form II to IV during the last 10 min of the experiment. The crystallization of CB into Form II as an initial polymorph at 20°C under static conditions reported here is in agreement with previous reports by van Malssen *et al*. (21) and Dewettinck *et al*. (22). However, the finding is in contrast to the report by MacMillan *et al*. (8,23) that the initial nucleating phase of CB during crystallization under static conditions at 20°C is Form III. The use of CB from different countries and also the difference in the experimental protocols may have caused the difference among the results from different works. In addition, it was apparent that Form III was not observed during the phase transition from Form II to Form IV of CB in this work. This is in contrast to a previous report (22) that shows the solid-state transformation from Form II to III and then to Form IV of CB crystallized at 20°C under static condition. Van Malssen *et al*. (21) show that a β′ polymorph exists in a "phase range" in which its X-ray diffraction pattern changes over a temperature range, depending on the cooling rate and crystallization temperature. This is due to the fact that CB is a mixture of TAG. It was possible that, after the initial solidification into Form II, the conditions for the crystallization performed in this experiment were only suitable for the β′ polymorph of the sample to exist in Form IV.

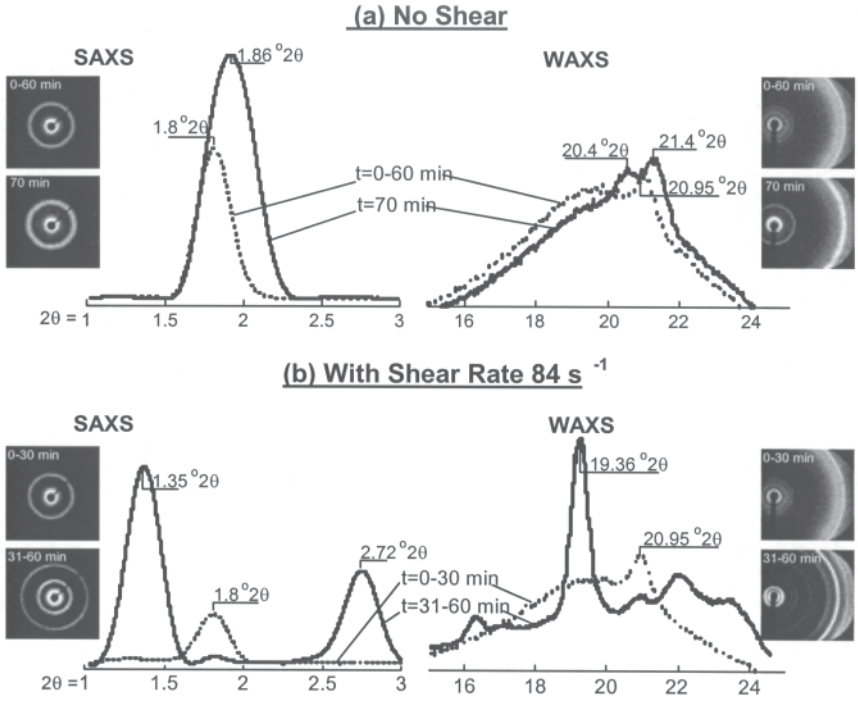

FIG. 3. X-ray diffraction patterns in small-angle X-ray scattering (SAXS) and wide-angle X-ray scattering (WAXS) of CB collected at different crystallization times at 20°C without shear and with shear rate 84 s^{-1}. The diffraction plots were derived from radial intensity averaging of the diffraction images captured by the detector. For abbreviation see Figure 1.

A series of experiments was carried out where shearing was superimposed during crystallization. With a wall shear rate of 84 s^{-1} (Fig. 3b), the sample solidified into Form II during the time 0–30 min with the same diffraction characteristics in both SAXS and WAXS as those of the crystallization without shear. However, at 31 min the sample structure began to exhibit significant changes. Two new diffraction peaks appeared in SAXS at 1.35°2θ (65.4 Å) and 2.72°2θ (32.5 Å), and one very sharp peak emerged in WAXS at 19.36°2θ (4.58 Å) accompanied by at least two smaller peaks on the larger 2θ side, which are characteristic of Form V (4). The existing diffraction peaks of Form II at 1.8°2θ and 20.95°2θ slowly disappeared. The changes in the diffraction patterns in both SAXS and WAXS indicated that the sample underwent a polymorphic transformation from Form II to V under the action of continuous shear.

In the experiments at shear rates 180, 240, 600, and 3000 s^{-1}, the samples exhibited a crystallization behavior similar to that at the shear rate condition at 84 s^{-1}; however, the kinetics of the transformation from Form II to V was modified as shown in Figure 4. The kinetics for the appearance and subsequent disappearance of Form II crystallization, together with the emergence of form V crystallization at all shear rates (0–3000 s^{-1}), are shown in the figure as a plot of the integrated intensity of Forms II and V vs. time. The integrated intensity, obtained from the area under the diffraction peak of a particular polymorphic form, is related to the amount of the solid phase in that form crystallized in the system (24). The time-dependent integrated intensity plots of different crystalline phases that coexist

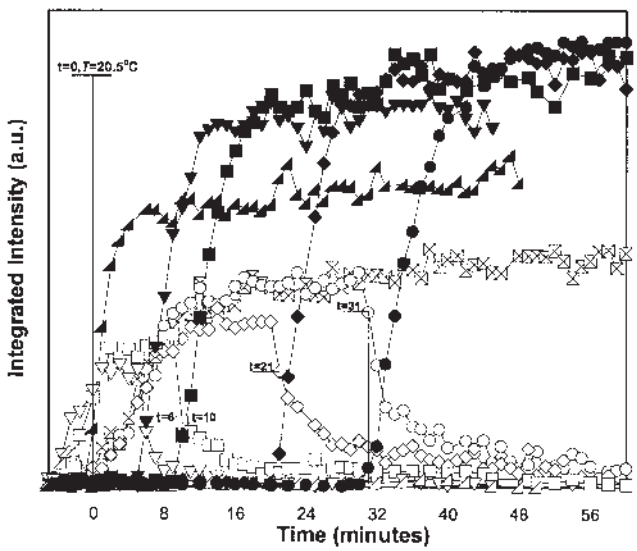

FIG. 4. Crystallization curves of Forms II and V of CB at 20°C under various shear rates. The curves are presented as a plot of integrated intensity, which was obtained from the area under the main diffraction peaks of Form II (at 1.8°2θ) and Form V (at 1.35°2θ), vs. time. (open box with superimposed ×, no shear in Form II; ○, shear rate 84 s^{-1} in Form II; ●, shear rate 84 s^{-1} in Form V; ◇, shear rate 180 s^{-1} in Form II; ◆, shear rate 180 s^{-1} in Form V; □, shear rate 240 s^{-1} in Form II; ■, shear rate 240 s^{-1} in Form V; ▽, shear rate 600 s^{-1} in Form II; ▼, shear rate 600 s^{-1} in Form V; open right triangle, lying on its side, shear rate 3000 s^{-1} in Form II; filled right triangle, lying on its side, shear rate 3000 s^{-1} in Form V). For abbreviation see Figure 1.

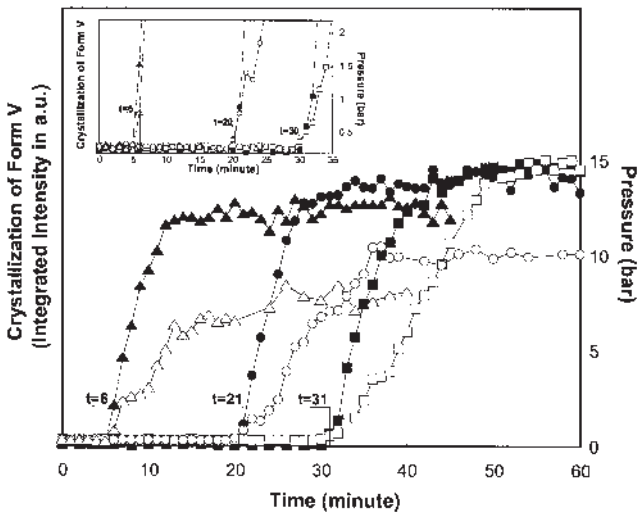

FIG. 5. The structure change (the crystallization of Form V in SAXS as presented by the integrated intensity) and the corresponding rheology change (the pressure difference) during the crystallization of CB at 20°C under various shear rates. The crystallization of Form V is represented by curves with closed symbols: ■, shear rate 84 s^{-1}; ●, shear rate 180 s^{-1}; ▲, shear rate 600 s^{-1}. The pressure difference is represented by curves with open symbols: □, shear rate 84 s^{-1}; ○, shear rate 180 s^{-1}; △, shear rate 600 s^{-1}. Insert shows the development at the early stages of Form V and the pressure difference on an enlarged y-scale. For abbreviations see Figures 1 and 3.

during crystallization with shear have been studied in depth for palm oil (25). At 20°C either without or with shear, CB always initially crystallized into Form II. At shear rates between 0 and 180 s^{-1}, the sample began to crystallize immediately as the temperature reached 20.5°C (at $t = 0$), implying that this shear rate range did not exhibit any significant effect on the onset of crystallization of Form II. However, at shear rates of 240 s^{-1} and higher, the fat started crystallization earlier. Without shear, the crystallization of Form II continued throughout 60 min. With shear, however, there appeared a time in each experiment when the development of Form II was interrupted by the formation of Form V. The crystallization of Form V at various shear rates started at different times as indicated in the figure. The time taken from when the temperature reached 20.5°C (at $t = 0$) to the point when Form V began to develop, the induction time of Form V, decreased from 31 to 21, 10, 6, and 0 min as the shear rate increased from 84 to 180, 240, 600, and 3000 s^{-1}, respectively. The shear-induced phase transition of CB from a less stable form to the more stable Form V is consistent with previous reports (8–10). Interestingly, the initial nucleating phase of CB crystallized under shear conditions at 20°C, which was identified as Form II in this work, was tentatively referred to by Mazzanti *et al*. (10) as Form II with the possible coexistence of Form III. All of this information is in contrast to the nucleating phase previously reported as Form III by MacMillan *et al*. (8). These authors used the X-ray diffraction technique in SAXS to study the crystallization of CB under shear. For the polymorphic structure of materials to be identified unambiguously, the diffraction characteristics in both SAXS and WAXS are required, and this was the technique we used in this work. The decrease in the induction time of Form V as the applied shear rate increased that is reported in this work is in agreement with a previous report (8). The phase transition of CB at 20°C from a less stable Form II to Form V at high shear rates between 600 and 3000 s^{-1} did not go through Form IV as reported for shear rate 720 s^{-1} by Mazzanti *et al*. (10). A possible explanation is the use of CB from different origins, hence with slightly different TAG compositions and different crystallization behavior.

During the studies of CB crystallization under continuous shear using the Rheo-X-Ray facility, the rheological changes (the pressure difference across the capillary) were also continuously monitored at the same time as the structure evolution. Here, the link between rheology changes and simultaneous structure changes of CB during crystallization can be developed. Figure 5 is a plot of the crystallization of Form V in SAXS and the associated pressure difference across the capillary of the MPR III vs. time for the crystallization at shear rates of 84, 180, and 600 s^{-1}. The samples in the three experiments had already crystallized into Form II from $t = 0$ (see Fig. 4). The pressure difference was low and relatively constant in all experiments as the sample crystallized into Form II. When the polymorphic transition from Form II to Form V occurred at later times (at $t = 31$, 21, and 6 min for the experiments with shear rates 84, 180, and 600 s^{-1}, respectively), the pressure difference began to increase sharply at nearly the same time as the development of Form V, before eventually attaining a plateau. Again, this pressure increase, which occurred in a similar pattern as the rapid increase in the complex viscosity under the action of shear step observe earlier (Fig. 2), was directly related to a viscosity increase of the sample, which was in turn linked to the amount of the Form V crystals formed.

Close examination of the data shows that the initial stages of development of Form V and pressure difference (insert of Fig. 5) did not necessarily occur at exactly the same time. In the experiments at shear rates of 84 and 180 s^{-1}, the increase in the pressure difference started slightly earlier (at $t = 30$ and 20 min, respectively) than that of the integrated intensity of Form V (at $t = 31$ and 21 min, respectively). It is possible that at the lower shear rates of 84 and 180 s^{-1}, the actual phase transition started slightly before it was detected in SAXS, leading to an earlier increase in the pressure difference than the integrated intensity of Form V. However, at a high shear rate of 600 s^{-1}, the phase transformation process was faster, resulting in the apparent spontaneous increase in both the pressure difference and the integrated intensity of Form V.

The effect of continuous shear on the crystal morphology and the crystallization kinetics of CB. Figure 6 shows CB crystals crystallized under static conditions at 20°C. Optically detectable nucleation took place after 2 min, where a few nuclei appeared within the isotropic and dark liquid background. At 5 min, the crystal number had increased, and some of the crystals began to develop into a spherulitic shape whereas newly formed crystals exhibited a long and narrow type of morphology. The shape of these newly formed crystals is similar to the

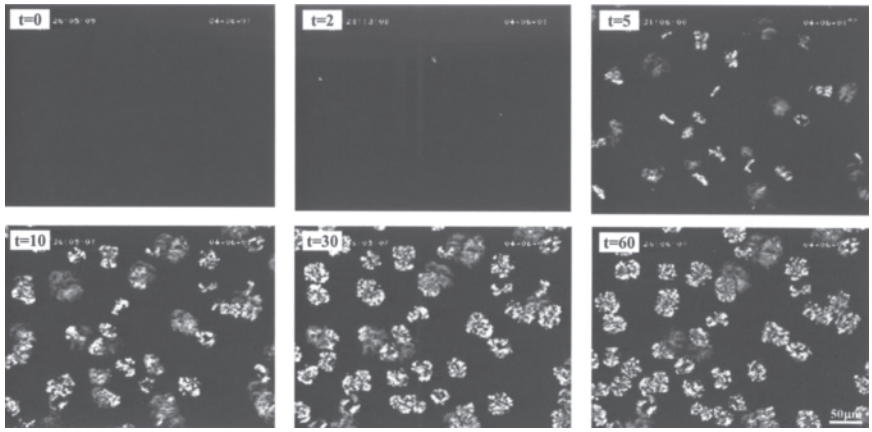

FIG. 6. CB crystals crystallized under quiescent conditions at 20°C (*t,* min). For abbreviation see Figure 1.

"bow-tie" or filamentous-shaped crystals formed during the early stages of static crystallization of CB reported by Manning and Dimick (26). At 10 min, the crystal number had increased slightly and most of the crystals had grown in size, indicating the domination of growth over nucleation. It can be seen that the crystals were generally of a spherulitic morphology, which were formed by agglomeration of smaller crystallites, but were not real spherulites because they did not exhibit the characteristic Maltese cross radial pattern (9). Toward the end of the experiment, the morphology of most of the crystals developed into spherulites and some crystals appeared attracted to each other, presumably by van der Waals forces (27,28) leading to some form of aggregation, which generally readily occurred as soon as the fat crystals attained a certain minimum size (28). It should be noted that at the end of the observed crystallization period a substantial fraction of uncrystallized material remained in the field of view.

The morphology of CB crystals crystallized with a low shear rate of 3 s^{-1} is shown in Figure 7. Overall, this shear rate did not significantly modify the morphology of individual crystals when compared with crystallization under static conditions. The first crystals started to appear at ~2 min. From this point on, the crystal number increased as time elapsed with a spherulitic growth development. However, in this experiment, there was a clear sign of crystal aggregation starting at 10 min. Between 30 and 60 min, the crystal size did not exhibit a significant increase. At 60 min, the size of the largest crystal in the image was obviously larger than the largest crystal in the experiment under static conditions at the same crystallization time. Crystal aggregation is common when fats crystallize under low shear or mild agitation (29). It is also known that aggregation is favored at high solids concentration and under conditions where the crystal–crystal collision is high (30). Mild shear applied to the sample during crystallization could increase the chance that the CB crystals come into contact with one another, after which they attach and form aggregates.

At a shear rate of 20 s^{-1} (Fig. 8), crystallization started at ~2 min. Between 5 and 10 min, the crystal number and the crystal size increased. Most crystals seemed to exhibit spherulitic growth. However, some crystals shown in the image did not develop in a spherulitic form. These crystals were small and appeared to be "crystal fragments," the morphology of which was a mixture of needle-like crystals and platelets. The spherulites seen in the images were clusters formed by agglomeration of

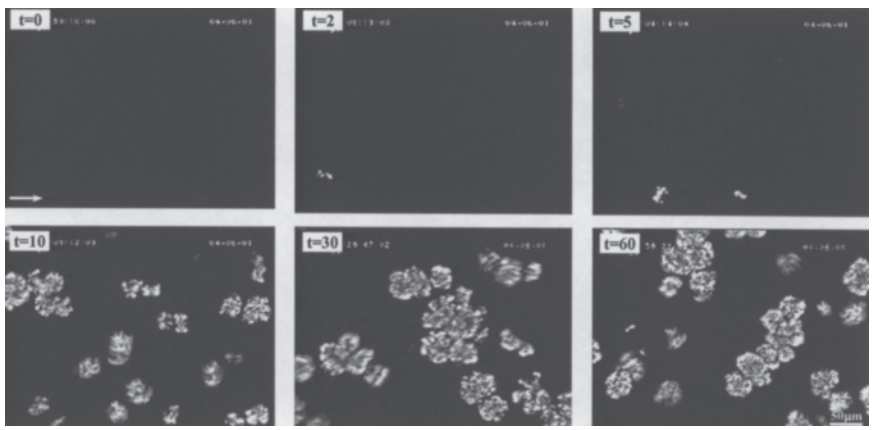

FIG. 7. CB crystals crystallized with shear rate 3 s^{-1} at 20°C. An arrow in the figure represents the direction of shear. For abbreviation see Figure 1.

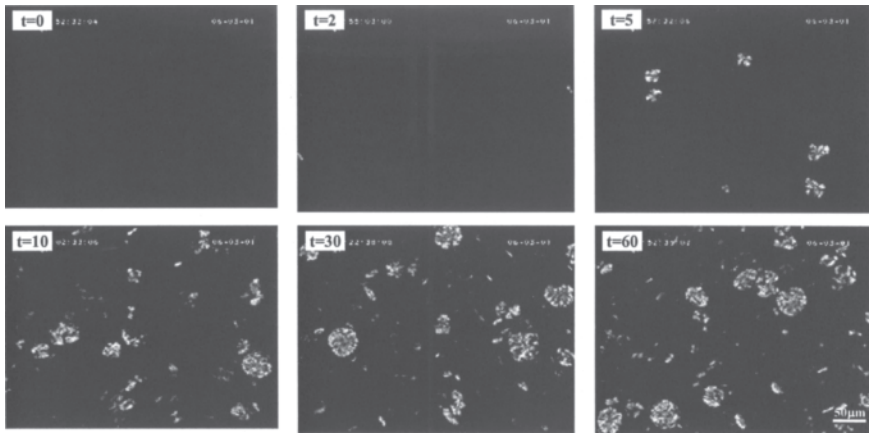

FIG. 8. CB crystals crystallized with shear rate 20 s^{-1} at 20°C. For abbreviation see Figure 1.

smaller crystallites with a random orientation (9). The application of shear rate 20 s^{-1} appears to prevent the formation of these spherulites to some extent, forcing some small crystallites to exist as individual crystal fragments, possibly with some degree of nonrandom distribution as suggested in the literature (9). There was no sign of crystal aggregation at this shear rate. This implies that, although the shear rate of 20 s^{-1} might have increased the collision rate, the forces generated due to shear possibly were sufficiently high to dominate the van der Waals attraction, and hence acted as destructive forces that prevented crystal aggregation.

At a shear rate of 100 s^{-1} (Fig. 9), the crystallization started at ~2 min. At 10 min, the existing crystals could be clearly seen to develop into two classes of crystal morphology: spherulites and crystal fragments. At this stage, it was not clear whether the crystals of these two morphologies were in the same or different polymorphic structures. Since CB crystals in one polymorphic form can exist in different types of morphology (26), it was hence possible that the polymorphic structures of the spherulites and the crystal fragments were the same.

At 57 min the sample suddenly transformed from a partly crystalline state, consisting of solid crystals suspended in the molten mother phase, to an almost completely solidified state. This sudden transformation is shown in detail in Figure 10. At 55 min, the crystal number was slightly higher than at 30 min (Fig. 9). However, only 1 min later, at 56 min, the number of the small crystal fragments increased rapidly. Both the number and size of the spherulites, on the other hand, were still approximately the same. At 56.5 min, the number of the crystal fragments had increased dramatically. By 57 min, the sample became almost fully crystallized, as judged by the optical appearance. The rapid contraction during the transformation of the sample resulted in the dark voids, which can be clearly seen in the image. The time ranges when the sample existed as crystals suspended in the liquid phase and as the nearly fully crystallized fat were defined here as the primary and secondary crystal growth periods, respectively. The transition of the sample from the primary to the secondary growth periods proceeded such that the primary spherulites appeared unmodified in either shape, number, or size. Instead, the images at 56.5 and 57 min show that during the transition the existing spherulites were quickly engulfed by the dominating small crystal fragments, which were rapidly increasing in number.

Shear rates of 300 and 500 s^{-1} in general exhibited effects on the crystallization kinetics of CB that were similar to those

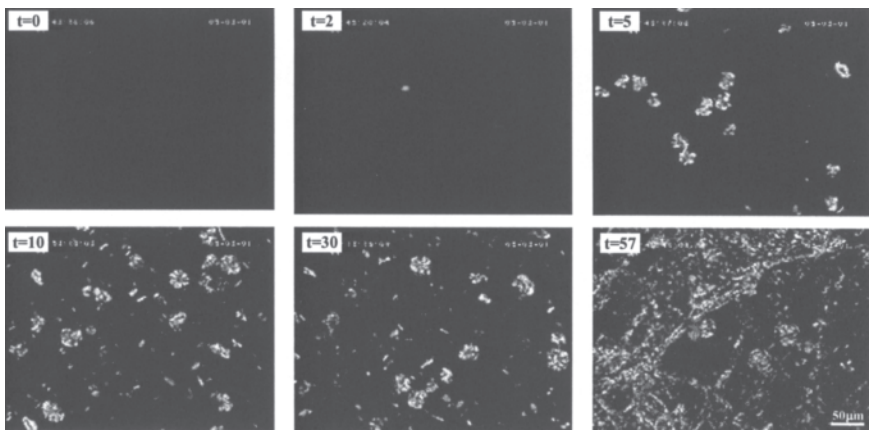

FIG. 9. CB crystals crystallized with shear rate 100 s^{-1} at 20°C. For abbreviation see Figure 1.

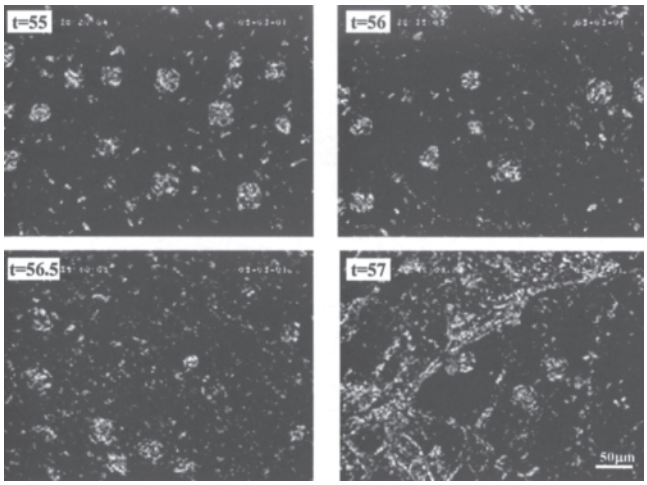

FIG. 10. The rapid increase in the number of crystals during the crystallization of CB at 20°C with shear rate 100 s^{-1} at crystallization times 55–57 min. For abbreviation see Figure 1.

at a shear rate of 100 s^{-1}, as can be seen in Figure 11. The effect of shear on the crystallization kinetics of CB observed through the optical techniques can be summarized as follow: (i) Only shear rates higher than 100 s^{-1} influenced the primary induction time crystallization. This is in agreement with the results from the Rheo-X-Ray technique, where the crystallization of the initial nucleating Form II started earlier at shear rates higher than 100 s^{-1} (Fig. 4). (ii) The primary-phase crystal number was not apparently affected by a low shear rate of 3 s^{-1} but was influenced by shear rates of 20 s^{-1} and higher, where the crystal number increased as the shear rate increased. (iii) The effect of shear on the crystal size was remarkable, especially when looking at the sizes of the spherulites. Compared with static conditions, the crystal size increased at a shear rate of 3 s^{-1}, was relatively unaffected by a shear rate of 20 s^{-1}, and decreased at shear rates of 100 s^{-1} and higher.

An increase in the crystal numbers during the crystallization of fats due to agitation has been reported (31,32). It is possible that some of the small crystal fragments as seen in the experiments under shear were broken pieces from spherulitic crystals that were generated during collisions among the spherulites. The increase and decrease in the crystal size of CB due to the low and high shear rates, respectively, were in agreement with what was observed during the crystallization of butterfat by Grall and Hartel (31) and milk fat by Herrera and Hartel (32,33). A possible explanation is that the collision between crystals in a mildly agitated or gently sheared sample could provide a potential for surface damage, which favors faster surface integration kinetics and leads to higher growth rate with increasing crystal size (34). In addition, low shear could reduce the chance of local temperature rise during the growth process of crystals. As a result, the local supercooling was maintained and so was the growth rate. Low shear could also enhance the possibility for the liquid molecules in the bulk to come in contact with and integrate into the crystal surface. However, at shear rates of 100 s^{-1}, the vigorous movement of the existing solid crystals inside the mother phase might make it difficult for the molecules to deposit onto the crystal surface and, as a consequence, the growth process would be decelerated.

The phenomenon of a rapid increase in the number of crystal fragments with a quick transformation into the solid phase when crystallized under a shear rate of 100 s^{-1} at 57 min was also observed with higher shear rates, but at earlier times: at 43 and 38 min for shear rates 300 and 500 s^{-1}, respectively (Fig. 11). This clearly suggests that the secondary crystallization of the fat occurred as a consequence of shear, and that the point in time at which it took place was strongly dependent on shear rate. It is probable that this point of abrupt increase in the crystal amount is the same point as the X-ray-detected phase transition from Form II to Form V where the sharp rise in the pressure difference has been observed (Fig. 5). If this is true, the polymorphic structure of the sample crystallized during the primary growth period in the CSS450 would be Form II, and of the sample within the secondary growth period would be Form V. To prove this was correct and also to correlate the results from all three experimental techniques to each other, X-ray characterization

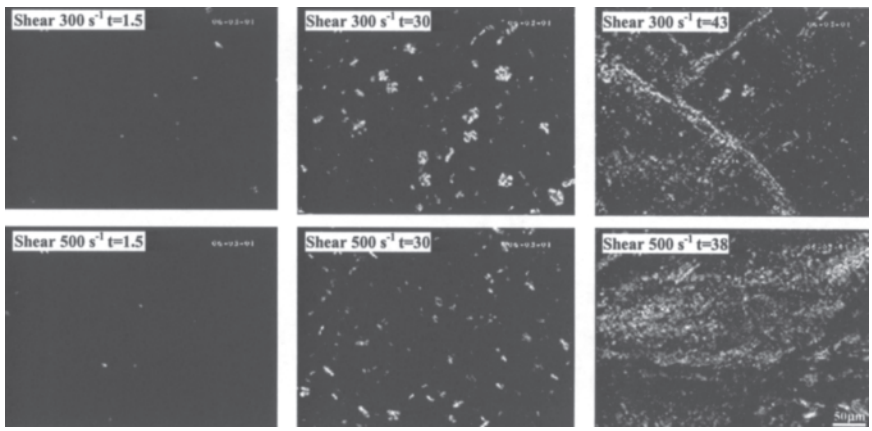

FIG. 11. CB crystals crystallized at 20°C with shear rates 300 s^{-1} (top row) and 500 s^{-1} (bottom row). For abbreviation see Figure 1.

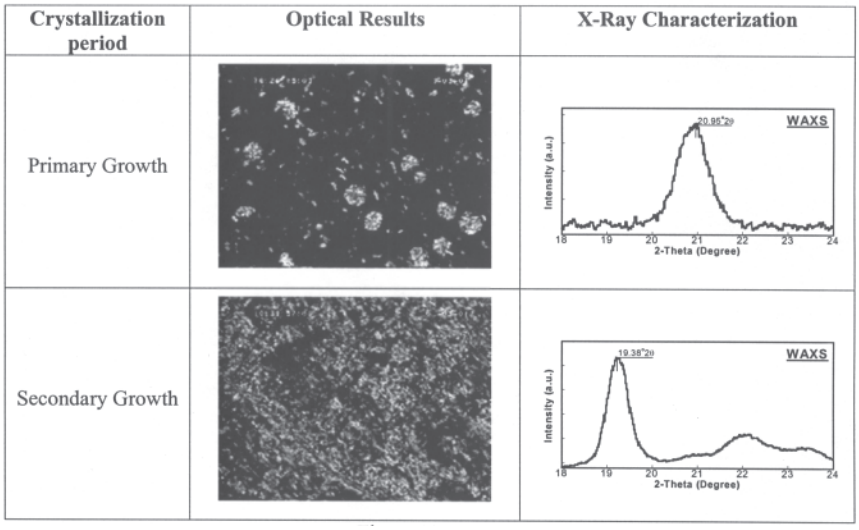

FIG. 12. Images of CB crystals crystallized at 20°C in the Cambridge Shear System (CSS450) at shear rate of 120 s^{-1} and the corresponding X-ray diffraction patterns in WAXS at times: (a) during the primary growth period (t = 30 min); (b) during the secondary growth period (t = 51 min). The diffraction plots were derived from radial intensity averaging of the diffraction images captured by the detector. For abbreviations see Figures 1 and 3.

was used to identify the polymorphic form of the sample from the two different growth periods. Two additional crystallization experiments were performed at 20°C with a shear rate of 120 s^{-1} using the CSS450. X-ray characterization of the sample from the test section of the microscope was performed at two different crystallization times: one during the primary growth period (at t = 30 min), the other during the secondary growth period (at about 1 min after the sample had transformed into an almost completely solidified fat). The results are shown in Figure 12. During the primary growth period, in which the sample partially crystallized into a mixture of spherulites and small crystal fragments, the X-ray characterization shows the diffraction pattern of solid CB in Form II only, with one diffraction peak at 20.95°2θ (4.24 Å). Once the crystallization of the sample had proceeded further into the secondary growth period with a rapid increase in crystallinity, the polymorphic structure of the sample was in Form V with one strong diffraction peak at 19.38°2θ (4.58 Å) and at least two more peaks on the larger 2θ side. The results exhibited in Figure 12 therefore confirm that the most remarkable effect of shear on the crystallization of CB at 20°C was the acceleration of polymorphic transformation from Form II to V (8–10,23), which occurred simultaneously with the dramatic change in crystal morphology, the substantial increase in the crystal amount, and the rapid transformation of the sample from a partially crystallized state into an almost completely solidified fat, as has been observed through the optical technique. This sudden increase in the crystal amount then caused the viscosity of the sample to rise sharply, resulting in the rapid increase of the pressure difference across the capillary observed through the rheological measurements using the MPR III. This shear-induced phase transition phenomenon therefore confirms the direct relationship between the viscosity and the crystallinity of CB during crystallization. This phenomenon, although it did not occur within the crystallization time of 60 min for shear rates as low as 3 and 20 s^{-1}, was to be expected if the experimental time was substantially extended. However, the expected induction time of Form V at shear rates of 3 s^{-1} would be larger than the one reported by MacMillan *et al.* (8). A possible explanation for the discrepancy is the use of shear cells with different configurations.

Kinetic analysis of Form V crystallization using the Avrami model. The crystallization kinetics of Form V as influenced by different shear rates was analyzed using the Avrami equation. The Avrami equation (35–37) is the most general approach for the description of isothermal phase transformation kinetics:

$$X(t) = 1 - \exp(-Bt^k) \quad [2]$$

where X is the fraction of material transformed at time t during crystallization, B is the Avrami rate constant, and k is the Avrami exponent. The equation describes the changes in the mass (or volume) of the crystals as a function of time during crystallization and is concerned with the overall crystallization process, including nucleation and growth (36). The Avrami rate constant B is a combination of nucleation and growth rate constants. The Avrami exponent k is a function of the number of dimensions in which growth takes place and provides qualitative information on the nature of the nucleation and growth processes (38). In this section, the crystallization curves of Form V were fitted to the linearized form of the Avrami equation by linear regression:

$$\ln[-\ln(1-X)] = \ln(B) + k\ln(t) \quad [3]$$

From Equation 3, a plot of $\ln[-\ln(1 - X)]$ vs. $\ln(t)$ has a slope of k and a y-intercept of $\ln(B)$.

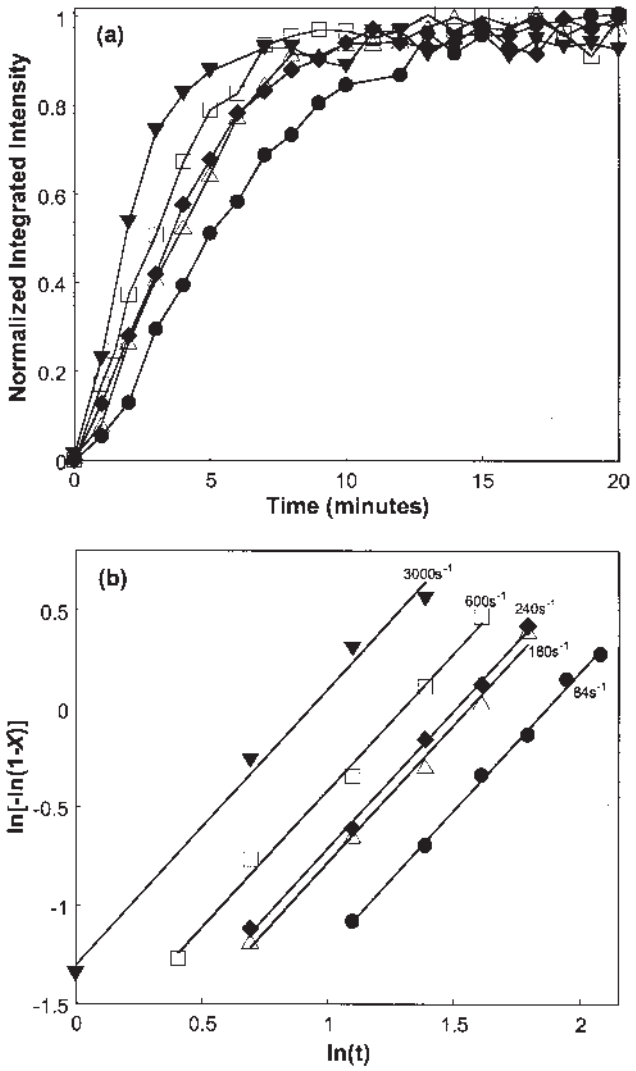

FIG. 13. (a) Normalized crystallization curves of Form V of CB obtained during crystallization at 20°C under various shear rates; (b) corresponding Avrami plots. (●, shear rate 84 s^{-1}; △, shear rate 180 s^{-1}; ◆, shear rate 240 s^{-1}; □, shear rate 600 s^{-1}; ▼, shear rate 3000 s^{-1}). For abbreviation see Figure 1.

The crystallization curves of Form V (Fig. 4) were modified and are presented in Figure 13a. In comparing the effect of shear on the crystallization kinetics of Form V during the initial stage of formation (where the integrated intensity increased rapidly) without taking into account the influence of the induction time on the Avrami exponent *k*, the induction time period has been removed from all modified crystallization curves. In addition, the crystallization curves have been normalized such that the maximum integrated intensity is ~1. The modified crystallization curves were fitted to the linearized form of the Avrami equation, and the results are shown in Figure 13b as Avrami plots ($R = 0.996–0.999$). The Avrami exponent *k* and the Avrami rate constant *B* were calculated and are given in Table 1. The crystallization of Form V at all shear rates exhibits approximately the same value of $k \cong 1.4$. Since this value of *k* was obtained without taking into account the influence of the induction time and was based on the approximate value of crystallinity, it does not conclusively represent the real nucleation and growth mechanism of Form V. Table 1, however, shows that the Avrami rate constant *B* increased with shear rate, indicating that crystallization of Form V was accelerated as the applied shear rate increased. This is in agreement with what was observed from Figure 13a where the crystallization curve of a higher shear rate is steeper during the rapid increase and takes less time to reach the plateau region.

TABLE 1
Avrami Exponent (*k*) and Avrami Rate Constant (*B*) for the Crystallization of Form V of Cocoa Butter at 20°C with Various Shear Rates[a]

Shear rate (s^{-1})	*k*	*B* (min^{-k})
84	1.41	7.18×10^{-2}
180	1.40	1.13×10^{-1}
240	1.40	1.21×10^{-1}
600	1.39	1.64×10^{-1}
3000	1.40	2.72×10^{-1}

[a]The *k* and *B* values were calculated from the slope and the y-intercept of the Avrami plots, respectively.

Development of overall physical model. In this paper, crystallization studies have been limited to one temperature alone, namely, 20°C. This was done for two reasons: first, the temperature provides a good experimental timescale for kinetic observation of crystallization events, and second, working at one crystallization temperature simplifies an already complex process. It should, however, be born in mind that events observed at 20°C do not necessarily match those found at different temperatures. In all cases, crystallization starts from the molten state as shown schematically in Figure 14 for crystallization with and without shear. Within the molten matrix, nucleation occurs in an unspecified way, and it has been established that this early crystallization is in Form II. From both the rheological and optical studies, it is clear that during the early period there is little change in the rheology of CB. From the optical observations, we estimate that the volume fraction of Form II crystals increases to a maximum of 2%, and we would therefore not expect a very large change in viscosity. At intermediate crystallization times a steady-state situation for crystal growth is observed where a dynamic equilibrium between the crystals and molten fraction is reached. However, this limiting level of crystallinity is not associated with spherulite impingement and subsequent consumption of all the CB. It is clear that a situation is reached where, at this temperature and timescale, only a certain amount of the CB is able to crystallize. Subsequent behavior depends very much on whether shear is applied during the whole crystallization process. If there is no shear, Form II spherulites transform to the more stable Form IV, although there appears to be no change in the optical morphology of the spherulites. The progressive transition to a more stable crystal form is to be expected, and it is possible that if the experimental time is substantially extended Form IV spherulites can transform into Form V.

The application of shear during crystallization had a very important effect. At early times, Form II nucleated and grew as a

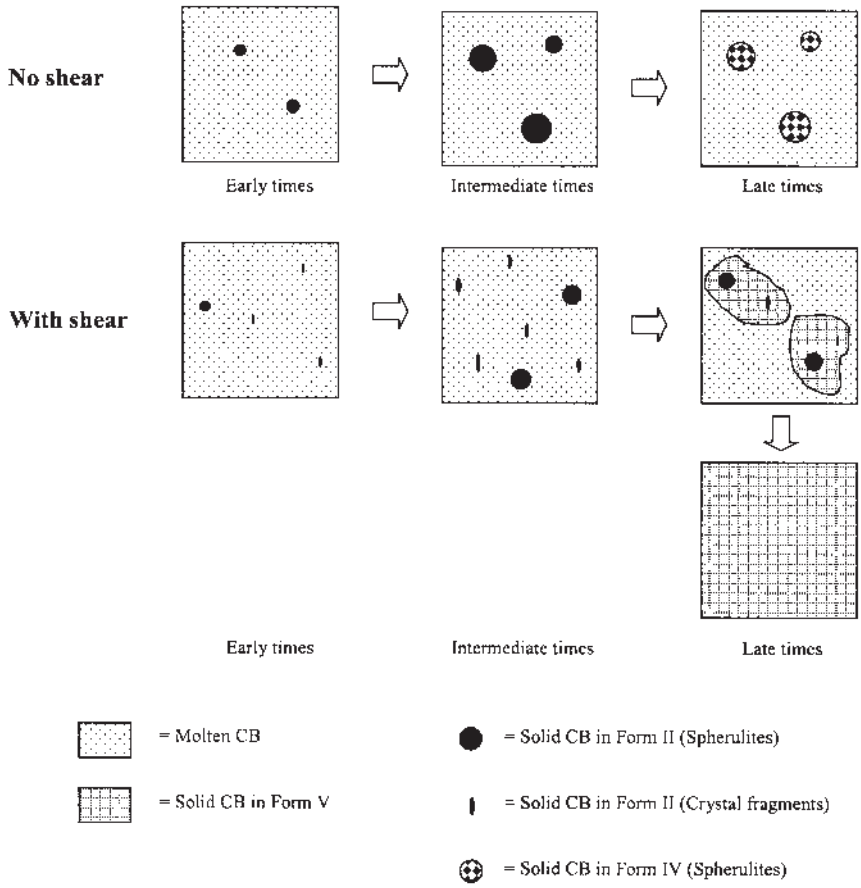

FIG. 14. Schematic diagram of CB crystallization kinetics: no shear and with shear. For abbreviation see Figure 1.

mixture of spherulites and crystal fragments. However, at a fairly precise time, which depended on the magnitude of the shear condition, a secondary nucleation and growth of Form V occurred and this rapidly dominated the crystallization kinetics. Within a few minutes of the onset of Form V visible nucleation, it appeared from optical observations that all the material had crystallized, and the X-ray data indicated saturation in Form V crystallization and also a disappearance of Form II crystal component. The emergence of the Form V component was very sensitive to the magnitude of the shear with the induction time decreasing with increasing shear conditions. The development of Form V crystallization matched a significant increase in the extrusion pressure for flow in the MPR III, and Form V crystallization appeared to result in either a high volume fraction of microcrystals with a significant enhancement in viscosity, or else the formation of intercalated network of crystals.

It is clear that shear promotes Form V crystallization, although at this stage we cannot provide any molecular insight as to why shear should promote the crystallization of this stable form. CB crystallization is complex and this work has shown that the superposition of shear effects kinetics, morphology, and polymorphic behavior. A single, simple, lumped-sum parameter is unable to describe the richness of changes that has been reported in this study. The schematic diagram shown in Figure 14 does, however, provide the basis from which quantitative modeling could be carried out. The results described in this paper should have relevance to the commercial tempering process, as shear is involved. However, tempering also involves a certain specific thermal profiling over a critical range of temperatures, which has not been examined in this work.

ACKNOWLEDGMENTS

The authors wish to acknowledge The Royal Thai Government for financial support and Nestlé PTC (York, England) for supplying CB samples used in this project. The authors also thank Dr. Steve Beckett of Nestlé PTC (York, England) for valuable advice and many useful discussions.

REFERENCES

1. Schlichter-Aronhime, J., and N. Garti, Solidification and Polymorphism in Cocoa Butter and the Blooming Problems, in *Crystallization and Polymorphism of Fats and Fatty Acids*, edited by N. Garti and K. Sato, Marcel Dekker, New York, 1988, pp. 363–393.
2. Dimick, P.S., Principles of Cocoa Butter Crystallization, *Manuf. Confect. 5*:109–114 (1991).
3. Chapman, D., The Polymorphism of Glycerides, *Chem. Rev. 62*:433–456 (1962).

4. Wille, R.L., and E.S. Lutton, Polymorphism of Cocoa Butter, *J. Am. Oil Chem. Soc. 43*:491–496 (1966).
5. Beckett, S.T., *The Science of Chocolate*, The Royal Society of Chemistry, Cambridge, 2000.
6. Nelson, R.B., Tempering, in *Industrial Chocolate Manufacture and Use*, 3rd edn., edited by S.T. Beckett, Blackie Academic & Professional, Oxford, 1999, pp. 231–258.
7. Feuge, R.O., W. Landmann, D. Mitcham, and N.V. Lovegren, Tempering Triglycerides by Mechanical Working, *J. Am. Oil Chem. Soc. 39*:310–313 (1962).
8. MacMillan, S.D., K.J. Roberts, A. Rossi, M.A. Wells, M.C. Polgreen, and I.H. Smith, *In Situ* Small Angle X-Ray Scattering (SAXS) Studies of Polymorphism with the Associated Crystallization of Cocoa Butter Fat Using Shearing Conditions, *Cryst. Growth Des. 2*:221–226 (2002).
9. Mazzanti, G., S.E. Guthrie, E.B. Sirota, A.G. Marangoni, and S.H.J. Idziak, Orientation and Phase Transitions of Fat Crystals Under Shear, *Ibid. 3*:721–725 (2003).
10. Mazzanti, G., S.E. Guthrie, E.B. Sirota, A.G. Marangoni, and S.H.J. Idziak, Novel Shear-Induced Phase in Cocoa Butter, *Ibid. 4*:409–411 (2004).
11. Ziegleder, G., Improved Crystallization Behaviour of Cocoa Butter Under Shearing, *Int. Z. Lebensm. Techn. Verfahrenst. 36*:412–418 (1985).
12. Toro-Vazquez, J.F., D. Perez-Martinez, E. Dibildox-Alvarado, M. Charo-Alonso, and J. Reyes-Hernandez, Rheometry and Polymorphism of Cocoa Butter During Crystallization Under Static and Shearing Conditions, *J. Am. Oil Chem. Soc. 81*:195–202 (2004).
13. Dhonsi, D., and A.G.F. Stapley, The Effect of Shear Rate, Temperature, Sugar and Emulsifer on the Tempering of Cocoa Butter, *J. Food Eng.*, in press.
14. deMan, J.M., and A.M. Beers, Fat Crystal Networks: Structure and Rheological Properties, *J. Texture Stud. 18*:303–318 (1987).
15. Saquet, O., G. Moggridge, and M.R. Mackley, Recent Development on the *In-Situ* Microstructural Characterisation of Flowing Soft-Solids and Polymers Using the Cambridge Multipass Rheometer, in *Proceedings of the 2nd European Congress of Chemical Engineering*, 1999.
16. Mackley, M.R., S. Wannaborwon, P. Gao, and F. Zhoa, The Optical Microscopy of Sheared Liquids Using a Newly Developed Optical Stage, *Microsc. Anal. 1*:25–27 (1999).
17. Mackley, M.R., R.T.J. Marshall, J. Smeulders, and F.D. Zhao, The Rheological Characterization of Polymeric and Colloidal Fluids, *Chem. Eng. Sci. 49*:2551–2565 (1994).
18. Ollivon, M., Triglycerides, in *Oils & Fats Manual: A Comprehensive Treatise. Volume I*, edited by A. Karleskind, Lavoisier Publishing, Paris, 1996, pp. 484–519.
19. Barnes, H.A., J.F. Hutton, and K. Walters, *An Introduction to Rheology*, Elsevier, Oxford, 1989.
20. Mackley, M.R., R.T.J. Marshall, and J. Smeulders, The Multipass Rheometer, *J. Rheol. 39*:1293–1309 (1995).
21. van Malssen, K.F., A. van Langevelde, R. Peschar, and H. Schenk, Phase Behavior and Extended Phase Scheme of Static Cocoa Butter Investigated with Real-Time X-Ray Powder Diffraction, *J. Am. Oil Chem. Soc. 76*:669–676 (1999).
22. Dewettinck, K., I. Foubert, M. Basiura, and B. Goderis, Phase Behavior of Cocoa Butter in a Two-Step Isothermal Crystallization, *Cryst. Growth Des. 4*:1295–1302 (2004).
23. MacMillan, S.D., K.J. Roberts, M.A. Wells, M.C. Polgreen, and I.H. Smith, Identification of the Initial Nucleating Form Involved in the Thermal Processing of Cocoa Butter Fat as Examined Using Wide Angle X-Ray Scattering (WAXS), *Ibid. 3*:117–119 (2003).
24. deMan, J.M., X-Ray-Diffraction Spectroscopy in the Study of Fat Polymorphism, *Food Res. Int. 25*:471–476 (1992).
25. Mazzanti, G., A.G. Marangoni, and S.H.J. Idziak, Modelling Phase Transitions During the Crystallization of a Multicomponent Fat Under Shear, *Phys. Rev. E 71-041607*:1–12 (2005).
26. Manning, D.M., and P.S. Dimick, Crystal Morphology of Cocoa Butter, *Food Microstruct. 4*:249–265 (1985).
27. Berger, K.G., G.G. Jewell, and R.J.M. Pollitt, Oils and Fats, in *Food Microscopy*, edited by J.G. Vaughan, Academic Press, New York, 1979, pp. 445–497.
28. Walstra, P., W. Kloek, and T. van Vliet, Fat Crystal Networks, in *Crystallization Processes in Fats and Lipid Systems*, edited by N. Garti and K. Sato, Marcel Dekker, New York, 2001, pp. 289–328.
29. Chaiseri, S., and P.S. Dimick, Dynamic Crystallization of Cocoa Butter: 2. Morphological, Thermal, and Chemical Characteristics During Crystal Growth, *J. Am. Oil Chem. Soc. 72*:1497–1504 (1995).
30. Bemer, G.G., and G. Smits, Industrial Crystallization of Edible Fats: Levels of Liquid Occlusion in Crystal Agglomerates, in *Proceedings of the 2nd World Congress of Chemical Engineering: Volume I*, 1981, pp. 369–371.
31. Grall, D.S., and R.W. Hartel, Kinetics of Butterfat Crystallization, *J. Am. Oil Chem. Soc. 69*:741–747 (1992).
32. Herrera, M.L., and R.W. Hartel, Effect of Processing Conditions on Physical Properties of a Milk Fat Model System, *Ibid. 77*:1177–1187 (2000).
33. Herrera, M.L., and R.W. Hartel, Effect of Processing Conditions on Physical Properties of a Milk Fat Model System: Microstructure, *Ibid. 77*:1197–1204 (2000).
34. Garside, J., and R.J. Davey, Secondary Contact Nucleation: Kinetics, Growth and Scale-Up, *Chem. Eng. Commun. 4*:393–424 (1980).
35. Avrami, M., Kinetics of Phase Change I: General Theory, *J. Chem. Phys. 7*:1103–1112 (1939).
36. Avrami, M., Kinetics of Phase Change II: Transformation-Time Relations for Random Distribution of Nuclei, *Ibid. 8*:212–224 (1940).
37. Avrami, M., Kinetics of Phase Change III: Granulation, Phase Change, and Microstructure, *Ibid. 9*:77–184 (1941).
38. Sharples, A., *Introduction to Polymer Crystallization*, Edward Arnold Publishers, London, 1966.

[Received September 8, 2005; accepted April 17, 2006]